

Fractional differential equations: non-constant coefficients, simulation and model reduction

Ruben Aylwin, Göksu Oruc, and Karsten Urban

Ulm University, Institute of Numerical Mathematics, Helmholtzstr. 20, 89081
Ulm, Germany

September 3, 2025

Abstract

We consider boundary value problems with Riemann-Liouville fractional derivatives of order $s \in (1, 2)$ with non-constant diffusion and reaction coefficients. A variational formulation is derived and analyzed leading to the well-posedness of the continuous problem and its Finite Element discretization. Then, the Reduced Basis Method through a greedy algorithm for parametric diffusion and reaction coefficients is analyzed. Its convergence properties, and in particular the decay of the Kolmogorov n -width, are seen to depend on the fractional order s . Finally, numerical results confirming our findings are presented.

1 Introduction

Differential equations with fractional derivatives have been widely studied in the literature, which is also due to the fact that those type of equations model phenomena, which are relevant in various fields. In this paper, we consider fractional order source problems with non-constant coefficients of the form

$$-{}_0\mathcal{D}_x^{\frac{s}{2}}\left(d(x){}_0\mathcal{D}_x^{\frac{s}{2}}u\right)+r(x)u(x)=f(x), \quad x \in \Omega := (0, 1), \quad (1.1a)$$

$$u(0)=0, u(1)=0, \quad (1.1b)$$

where $u : \Omega \rightarrow \mathbb{R}$ denotes the unknown function, ${}_0\mathcal{D}_x^{\beta}$ is the left-sided Riemann-Liouville fractional derivative of order $\beta > 0$, $s \in (1, 2)$ is the order of the fractional differential equation, $r : \Omega \rightarrow \mathbb{R}$ is the reaction coefficient, $d : \Omega \rightarrow \mathbb{R}$ is the diffusion coefficient and $f : \Omega \rightarrow \mathbb{R}$ is the right-hand side.

Systems like eq. (1.1) have been studied in [14] for the case of constant diffusion, i.e., $d \equiv 1$. We are interested in the more general case also since the fractional operator in eq. (1.1a) appears, for example, when considering the fractional Fick's law of diffusion [24] together with fractional conservation of mass [28]. Different operators involving non-constant coefficients have been considered also in [17, 27], while applications of fractional derivatives include sub-diffusive [13, 19] and super-diffusive [16] processes, which also motivate the present article.

One source of motivation for this paper is model reduction for problems of fractional order. Since those kind of problems are non-local, model reduction might offer additional potential for reduction. To this end, we consider a parameterized version of eq. (1.1), where d , r and the right-hand side f may vary depending on values of parameters $\mu \in \mathcal{P}$, where $\mathcal{P} \subset \mathbb{R}^P$. One might think of a material with different diffusion coefficients in different areas. The Reduced Basis Method (RBM) is a well-established model order reduction technique for parameterized partial differential equations (PPDEs), see e.g. [5, 10, 11, 21, 26]. We aim at extending the RBM to fractional-type problems. The RBM relies on a well-posed variational formulation of the parameterized problem.

Hence, we aim at generalizing the results for constant coefficients in [14] to the non-constant coefficient case.

The next ingredient for the RBM is a “truth” solver which is able to determine the solution of the problem for a given value of the parameter up to any desired accuracy. Those detailed solutions (also called “snapshots”) are used in an offline training phase to derive a reduced model by maximizing an error estimator w.r.t. a finite training subset $\mathcal{P}_{\text{train}} \subset \mathcal{P}$ of parameters in a greedy manner. Hence, an efficiently computable and sharp error estimator is needed, which can be formed by the inverse of the coercivity constant multiplied by the dual norm of the residual. This is the reason why we derive a formula for the coercivity constant as this also makes the dependency of the fractional order s explicit.

The best possible error that can be achieved by the RBM of size $n \in \mathbb{N}$ is given by the *Kolmogorov n -width* $d_n(\mathcal{P})$. It is known that $d_n(\mathcal{P})$ decays exponentially fast for elliptic and (space-time variational) parabolic problems, but may show very poor decay for transport and wave-type phenomena, see e.g. [1, 20]. Hence, we are interested how $d_n(\mathcal{P})$ behaves w.r.t. the fractional order s as $s \rightarrow 2$ is expected to show elliptic and $s \rightarrow 1$ transport-type behavior.

The remainder of this paper is organized as follows. In Section 2 we collect some notation and known facts on the Riemann-Liouville fractional operators. We also derive a norm equivalence in Lemma 2.10, which is crucial for the subsequent analysis. Section 3 is devoted to the derivation and the analysis of a variational formulation for fractional differential equations with non-constant coefficients, as well as their solutions, extending the results in [14]. A Finite Element discretization is presented and analyzed in Section 4. We describe the application of the RBM for parameterized diffusion and reaction coefficients in Section 5. Whereas the application of the RBM turns out to be rather standard (since a coercive variational formulation has been derived in Section 3 before), the analysis of the decay of the Kolmogorov n -width w.r.t. the fractional order s in Section 5.4 is (to the very best of our knowledge) new. Numerical experiments both for the FEM and the RBM are presented in Section 6. We close with some conclusions and an outlook in Section 7.

2 Some facts on Fractional Differential Operators

2.1 Notation

Let U be a Banach space with norm $\|\cdot\|_U$ and dual space U' . The space of bounded linear operators between two Banach spaces U and V is written as $\mathcal{L}(U, V)$. For a Hilbert space H , we let $(\cdot, \cdot)_H$ and $\langle \cdot, \cdot \rangle_{H' \times H}$ denote its inner and duality products, respectively. Since we will be dealing mostly with spaces of real-valued functions, all inner and duality products are understood in the bilinear sense.

For $m \in \mathbb{N}$ and an open and bounded Lipschitz domain $\Omega \in \mathbb{R}^d$, $d \in \{1, 2, 3\}$, the space of real valued continuous functions on Ω with m continuous derivatives in Ω is denoted by $C^m(\Omega)$, $C^\infty(\Omega)$ is the space of infinitely continuously differentiable functions in Ω and $C_0^\infty(\Omega)$ is the space of functions in $C^\infty(\Omega)$ with compact support in Ω . Furthermore, for $p \geq 1$, the usual space of p -integrable measurable functions over Ω is denoted by $L_p(\Omega)$ and, for $s \in \mathbb{R}$, we use the Sobolev spaces (of broken order) $H^s(\Omega)$, $H_0^s(\Omega)$ and $\tilde{H}^s(\Omega)$ as in [18] and recall the duality relationships

$$H^s(\Omega)' = \tilde{H}^{-s}(\Omega) \quad \text{and} \quad \tilde{H}^s(\Omega)' = H^{-s}(\Omega),$$

as well as the equivalence

$$\tilde{H}^s(\Omega) = H_0^s(\Omega), \quad \forall s \geq 0 \text{ such that } s \notin \{\frac{1}{2}, \frac{3}{2}, \dots\},$$

with equivalent norms (c.f. [18, Thm. 3.33]). The semi-norm of the Sobolev space of order $s > 0$ is written as $|\cdot|_{H^s(\Omega)}$. We will always identify the space $L_2(\Omega)$ with its dual, so as to obtain Gelfand triples $\tilde{H}^{-s}(\Omega) \hookrightarrow L_2(\Omega) \hookrightarrow H^s(\Omega)$ and $H^{-s}(\Omega) \hookrightarrow L_2(\Omega) \hookrightarrow \tilde{H}^s(\Omega)$. Furthermore, we will be required to work with Sobolev spaces of functions over Ω that have smooth extensions by

zero to the left and right sides of Ω , defined as

$$\begin{aligned}\tilde{H}_L^s(\Omega) &:= \{u \in H^s(\Omega) : \exists \tilde{u} \in \tilde{H}^s(0, \infty) \text{ s.t. } u = \tilde{u}|_\Omega\}, \\ \tilde{H}_R^s(\Omega) &:= \{u \in H^s(\Omega) : \exists \tilde{u} \in \tilde{H}^s(-\infty, 1) \text{ s.t. } u = \tilde{u}|_\Omega\}.\end{aligned}$$

A Hilbert space structure is recovered for $\tilde{H}_L^s(\Omega)$ by restricting the norm and product of $H^s(-\infty, 1)$ to left-sided extension by zero of elements in $\tilde{H}_L^s(\Omega)$. Analogously, restricting the norm and product of $H^s(0, \infty)$ to the right-sided extension by zero of elements in $\tilde{H}_R^s(\Omega)$ yields the corresponding Hilbert space structure for this space. These spaces were introduced in [14, §2] and characterize the range and domain of fractional integral and differential operators to be defined later on. Furthermore, consider the spaces

$$\begin{aligned}C_L^\infty(\Omega) &:= \{u = \tilde{u}|_\Omega \text{ for some } \tilde{u} \in C_0^\infty(0, \infty)\}, \\ C_R^\infty(\Omega) &:= \{u = \tilde{u}|_\Omega \text{ for some } \tilde{u} \in C_0^\infty(-\infty, 1)\}.\end{aligned}$$

By proceeding analogously as in [18, Chap. 3.6], one can see that these spaces are dense in $\tilde{H}_L^s(\Omega)$ and $\tilde{H}_R^s(\Omega)$, respectively. Furthermore, we shall identify elements of $\tilde{H}^s(\Omega)$, $\tilde{H}_L^s(\Omega)$ and $\tilde{H}_R^s(\Omega)$ with their corresponding extensions by 0 so as to not introduce additional notation.

Finally, \mathcal{F} will denote the Fourier transform, Γ will correspond to the Gamma function, and $\lceil s \rceil$ and $\lfloor s \rfloor$ will denote, for any $s \in \mathbb{R}$, the smallest integer larger than s and the largest integer smaller than s , respectively.

2.2 Fractional Operators

2.2.1 Fractional Integral Operators

We begin by introducing the Riemann-Liouville fractional integral operators of order $s > 0$, which are needed for the construction of fractional differential operators (*c.f.* [22, Chap. 1.2.3] and [15, §2.1]).

Definition 2.1 (Fractional Integral Operators). *For any $s > 0$, $\varphi \in L_1(0, \infty)$ and $\psi \in L_1(-\infty, 1)$, we introduce the left- and right-sided Riemann-Liouville fractional integral operators as*

$$\begin{aligned}_0\mathcal{I}_x^s\varphi(x) &:= \frac{1}{\Gamma(s)} \int_0^x (x-t)^{s-1}\varphi(t)dt \quad \forall x > 0, \\ {}_x\mathcal{I}_1^s\psi(x) &:= \frac{1}{\Gamma(s)} \int_x^1 (t-x)^{s-1}\psi(t)dt \quad \forall x < 1.\end{aligned}$$

The following lemmas introduce useful properties of the integral operators, which have appeared in [14, 15, 22]. We omit the proofs for brevity, but point out relevant references for each result. We also refer to [15, La. 2.1 and 2.3] for more details.

Lemma 2.2 ([22, Thm. 2.6]). *The fractional integral operators introduced in Definition 2.1 are bounded in $L_p(\Omega)$, $\Omega = (0, 1)$, for any $p \geq 1$, with continuity constant $1/\Gamma(s+1)$. Moreover, for any $s_1, s_2 > 0$ and $\varphi \in L_p(\Omega)$ they satisfy $_0\mathcal{I}_x^{s_1+s_2}\varphi = _0\mathcal{I}_x^{s_2}{}_0\mathcal{I}_x^{s_1}\varphi$ and ${}_x\mathcal{I}_1^{s_1+s_2}\varphi = {}_x\mathcal{I}_1^{s_2}{}_x\mathcal{I}_1^{s_1}\varphi$. \square*

Lemma 2.3 ([14, Thm. 3.1 and Rem. 3.1]). *Let $s, \sigma \geq 0$. The fractional integral operators $_0\mathcal{I}_x^s$ and ${}_x\mathcal{I}_1^s$ are bounded from $\tilde{H}_L^\sigma(\Omega)$ to $\tilde{H}_L^{\sigma+s}(\Omega)$ and from $\tilde{H}_R^\sigma(\Omega)$ to $\tilde{H}_R^{\sigma+s}(\Omega)$, respectively. \square*

Lemma 2.4 ([22, Cor. to Thm. 3.5]). *Let $s \geq 0$. For any $\psi, \phi \in L_2(\Omega)$ the following relation holds $(_0\mathcal{I}_x^s\psi, \phi)_{L_2(\Omega)} = (\psi, {}_x\mathcal{I}_1^s\phi)_{L_2(\Omega)}$. \square*

2.2.2 Fractional Differential Operators

We are now ready to introduce the fractional Riemann-Liouville derivatives and their properties.

Definition 2.5 (Fractional Derivatives). *For any non-integer $s > 0$, $\varphi \in C_L^\infty(\Omega)$ and $\psi \in C_R^\infty(\mathbb{R})$, we introduce the left-sided ${}_0\mathcal{D}_x^s$ and right-sided ${}_x\mathcal{D}_1^s$ Riemann-Liouville fractional derivative for all $x \in \Omega$ as*

$${}_0\mathcal{D}_x^s\varphi(x) := \frac{d^{\lceil s \rceil}}{dx^{\lceil s \rceil}} \left({}_0\mathcal{I}_x^{\lceil s \rceil - s}\varphi(x) \right) \quad \text{and} \quad {}_x\mathcal{D}_1^s\psi(x) := -\frac{d^{\lceil s \rceil}}{dx^{\lceil s \rceil}} \left({}_x\mathcal{I}_1^{\lceil s \rceil - s}\psi(x) \right).$$

Identifying $\varphi \in \tilde{H}^s(\Omega)$ with its zero extension to \mathbb{R} allows us to extend the fractional derivatives to the outside of Ω as well.

Lemma 2.6 ([14, Thm. 2.2]). *For any $s > 0$ the fractional differential operators ${}_0\mathcal{D}_x^s$ and ${}_x\mathcal{D}_1^s$ have bounded extensions from $\tilde{H}_L^s(\Omega)$ and $\tilde{H}_R^s(\Omega)$ to $L_2(\Omega)$, respectively. Moreover, $\|{}_0\mathcal{D}_x^s\varphi\|_{L_2(\Omega)} \leq \|\varphi\|_{\tilde{H}_L^s(\Omega)}$ for all $\varphi \in \tilde{H}_L^s(\Omega)$ and $\|{}_x\mathcal{D}_1^s\psi\|_{L_2(\Omega)} \leq \|\psi\|_{\tilde{H}_R^s(\Omega)}$ for all $\psi \in \tilde{H}_R^s(\Omega)$. \square*

Lemma 2.7 ([8, Prop. A.4] or [22, Thm. 2.4]). *The left and right-sided fractional derivatives of order $s > 0$ act as left inverses of the left- and right-sided fractional integral operators of order s , i.e., ${}_0\mathcal{D}_x^s{}_0\mathcal{I}_x^s\varphi(x) = \varphi(x)$ and ${}_x\mathcal{D}_1^s{}_x\mathcal{I}_1^s\psi(x) = \psi(x)$, whenever $\varphi(x)$ is a summable function. \square*

Lemma 2.8 ([14, La. 4.1]). *Let $s \in (0, 1)$. Then, for all $x \in \Omega$ it holds ${}_0\mathcal{D}_x^s\varphi(x) = {}_0\mathcal{I}_x^{1-s}\varphi'(x)$ for all $\varphi \in C_L^\infty(\Omega)$ and ${}_x\mathcal{D}_1^s\psi(x) = -{}_x\mathcal{I}_1^{1-s}\psi'(x)$ for $\psi \in C_R^\infty(\Omega)$. Furthermore, these relationships can be extended to hold for $\varphi \in \tilde{H}_L^1(\Omega)$ and $\psi \in \tilde{H}_R^1(\Omega)$, respectively. \square*

The next statement is a generalization of integration by parts and is fundamental for the subsequent derivation of a variational formulation.

Proposition 2.9 ([14, §4.1]). *Let $\varphi \in C_L^\infty(\Omega)$, $\psi \in C_R^\infty(\Omega)$ and $s \in (0, 1)$. Then, $({}_0\mathcal{D}_x^s\varphi(x), \psi(x))_{L_2(\Omega)} = (\varphi(x), {}_x\mathcal{D}_1^s\psi(x))_{L_2(\Omega)}$.*

2.3 Equivalent Norms in $\tilde{H}^s(\Omega)$

We continue by analyzing equivalent norms in $\tilde{H}^s(\Omega)$ that will facilitate our analysis of variational formulations of FPDEs.

Lemma 2.10. *Let $s > 0$, $s \notin \{\frac{1}{2}, \frac{3}{2}, \dots\}$. Then, for $\varphi \in \tilde{H}^s(\Omega)$ we have the relation $({}_0\mathcal{D}_x^s\varphi, {}_x\mathcal{D}_1^s\varphi)_{L_2(\Omega)} = \cos(\pi s) \|{}_0\mathcal{D}_x^s\varphi\|_{L_2(\mathbb{R})}^2 = \cos(\pi s) \|{}_x\mathcal{D}_1^s\varphi\|_{L_2(\mathbb{R})}^2$.*

Proof. The proof follows from [8, Thm. 2.3, Lem. 2.4]. \square

Proposition 2.11. *Set $\|\varphi\|_s := (\|\varphi\|_{L_2(\Omega)}^2 + \|{}_0\mathcal{D}_x^s\varphi\|_{L_2(\mathbb{R})}^2)^{\frac{1}{2}}$ as well as $|\varphi|_s := \|{}_0\mathcal{D}_x^s\varphi\|_{L_2(\mathbb{R})}$. Then, for all $\varphi \in \tilde{H}^s(\Omega)$,*

$$\|\varphi\|_{\tilde{H}^s(\Omega)} \leq \|\varphi\|_s \leq \sqrt{2} \|\varphi\|_{\tilde{H}^s(\Omega)}, \quad \frac{\Gamma(s+1)}{\sqrt{2}} \|\varphi\|_{\tilde{H}^s(\Omega)} \leq |\varphi|_s \leq \|\varphi\|_{\tilde{H}^s(\Omega)}. \quad (2.1)$$

Proof. By consequence of [8, Thm. 2.10] together with Lemma 2.2 we have that $\|\varphi\|_{L_2(\Omega)} \leq \Gamma(s+1)^{-1} \|{}_0\mathcal{D}_x^s\varphi\|_{L_2(\Omega)}$ for all $\varphi \in \tilde{H}_L^s(\Omega)$. Further considering $\varphi \in C_0^\infty(\Omega)$, we have that

$$2 \|{}_0\mathcal{D}_x^s\varphi\|_{L_2(\mathbb{R})}^2 \geq \Gamma(s+1)^2 \|\varphi\|_{L_2(\Omega)}^2 + \|{}_0\mathcal{D}_x^s\varphi\|_{L_2(\mathbb{R})}^2 \geq \Gamma(s+1)^2 \|\varphi\|_s^2,$$

where we have used that $\Gamma(x) < 1$ for $x \in (1, 2)$. Next, we use

$$\mathcal{F}({}_0\mathcal{D}_x^s\varphi)(\omega) = (-i\omega)^s \mathcal{F}(\varphi)(\omega) \quad \text{for } \varphi \in C_0^\infty(\mathbb{R}) \quad (2.2)$$

(see, e.g. [15, Rem. 2.11]) to deduce

$$\|\varphi\|_s^2 = \int_{\mathbb{R}} (1 + |\omega|^{2s}) |\mathcal{F}(\varphi)(\omega)|^2 d\omega \geq \int_{\mathbb{R}} (1 + |\omega|^2)^s |\mathcal{F}(\varphi)(\omega)|^2 d\omega = \|\varphi\|_{H^s(\mathbb{R})}^2.$$

In addition, we have that $\|\varphi\|_{H^s(\mathbb{R})} \leq \sqrt{2}\Gamma(s+1)^{-1}\|{}_0\mathcal{D}_x^s\varphi\|_{L_2(\mathbb{R})}$, i.e., the left-handed inequalities in (2.1) for all $\varphi \in C_0^\infty(\Omega)$. Since $C_0^\infty(\Omega)$ is dense in $\tilde{H}^s(\Omega)$, we can conclude the estimates also for $\varphi \in \tilde{H}^s(\Omega)$. Concerning the upper bounds, consider $\varphi \in C_L^\infty(\Omega)$ and, by the Plancherel's theorem and (2.2) we get that

$$\begin{aligned}\|{}_0\mathcal{D}_x^s\varphi\|_{L_2(\Omega)} &\leq |\varphi|_s = \|{}_0\mathcal{D}_x^s\varphi\|_{L_2(\mathbb{R})} = \|\mathcal{F}({}_0\mathcal{D}_x^s\varphi)(\omega)\|_{L_2(\mathbb{R})} = \|(-i\omega)^s\mathcal{F}(\varphi)(\omega)\|_{L_2(\mathbb{R})} \\ &= \int_{\mathbb{R}} |\omega|^{2s} |\mathcal{F}(\varphi)(\omega)|^2 d\omega \leq \int_{\mathbb{R}} (1 + |\omega|^2)^s |\mathcal{F}(\varphi)(\omega)|^2 d\omega = \|\varphi\|_{H^s(\mathbb{R})}.\end{aligned}$$

The remaining claims follow as in the proofs of [14, Thm. 2.1 and 2.2]. \square

3 Riemann-Liouville Fractional Problem

We continue by deriving a variational formulation for (1.1) (which, to the best of our knowledge, has not been considered before) and analyze its well-posedness and smoothness of its solutions.

3.1 Variational Formulation

We shall work under the following assumptions on the data:

Assumption 3.1. *Let $s \in (1, 2)$, $d \in L_\infty(\Omega)$ such that $d(x) \geq d_0 > 0$ for almost all $x \in \Omega$, $r \in L_\infty(\Omega)$ and $f \in L_2(\Omega)$.*

Then, we shall consider the fractional differential operator with non-constant diffusion coefficients as

$$\mathcal{D}_d^s u(x) := {}_0\mathcal{D}_x^{\frac{s}{2}} \left(d(x) {}_0\mathcal{D}_x^{\frac{s}{2}} u(x) \right), \quad (3.1)$$

As mentioned in Section 1, similar operators were studied in [17]—where the innermost left-sided derivative in eq. (1.1a) is replaced by a right-sided derivative—and in [27]—where the coefficient stands “outside” of the fractional derivative, i.e., $\frac{d}{dx}(d(x) {}_0\mathcal{D}_x^{s-1} u(x))$. Both choices lead to milder conditions on the parameter $d(x)$ for the well-posedness of the considered variational formulations.

We begin by considering the left-hand side of eq. (1.1a) with $u \in C_0^\infty(\Omega)$. Multiplication with a test function $v \in C_0^\infty(\Omega)$ and integration over Ω yields

$$-(\mathcal{D}_d^s u, v)_{L_2(\Omega)} + (r u, v)_{L_2(\Omega)}. \quad (3.2)$$

Applying Proposition 2.9 yields,

$$-(\mathcal{D}_d^s u, v)_{L_2(\Omega)} = -\left({}_0\mathcal{D}_x^{\frac{s}{2}} \left(d_0 {}_0\mathcal{D}_x^{\frac{s}{2}} u \right), v\right)_{L_2(\Omega)} = -\left(d_0 {}_0\mathcal{D}_x^{\frac{s}{2}} u, {}_x\mathcal{D}_1^{\frac{s}{2}} v\right)_{L_2(\Omega)}.$$

Therefore, given Assumption 3.1, we introduce the following bilinear and linear forms

$$a(u, v) := -\left(d_0 {}_0\mathcal{D}_x^{\frac{s}{2}} u, {}_x\mathcal{D}_1^{\frac{s}{2}} v\right)_{L_2(\Omega)} + (r u, v)_{L_2(\Omega)} =: a_1(u, v) + a_2(u, v), \quad (3.3)$$

$$F(v) := (f, v)_{L_2(\Omega)}. \quad (3.4)$$

Problem 3.2. *Seek $u \in \tilde{H}^{\frac{s}{2}}(\Omega)$ such that $a(u, v) = F(v)$ for all $v \in \tilde{H}^{\frac{s}{2}}(\Omega)$.*

To investigate the well-posedness of Problem 3.2, we need some preparations.

Lemma 3.3. *If Assumption 3.1 holds, the bilinear form in eq. (3.3) is continuous in $\tilde{H}^{\frac{s}{2}}(\Omega)$, i.e., with $C_{d,r} := 2(\|d\|_{L_\infty(\Omega)} + \|r\|_{L_\infty(\Omega)})$*

$$a(u, v) \leq C_{d,r} \|u\|_{\tilde{H}^{s/2}(\Omega)} \|v\|_{\tilde{H}^{s/2}(\Omega)} \quad \forall u, v \in \tilde{H}^{\frac{s}{2}}(\Omega).$$

Proof. Clearly, for $u, v \in \tilde{H}^{\frac{s}{2}}(\Omega)$, it holds that

$$\begin{aligned} a_1(u, v) &\leq \|d\|_{L_\infty(\Omega)} \left| \left({}_0\mathcal{D}_x^{\frac{s}{2}} u, {}_x\mathcal{D}_1^{\frac{s}{2}} v \right)_{L_2(\Omega)} \right| \leq \|d\|_{L_\infty(\Omega)} \|{}_0\mathcal{D}_x^{\frac{s}{2}} u\|_{L_2(\Omega)} \|{}_x\mathcal{D}_1^{\frac{s}{2}} v\|_{L_2(\Omega)} \\ &\leq \|d\|_{L_\infty(\Omega)} \|{}_0\mathcal{D}_x^{\frac{s}{2}} u\|_{L_2(\mathbb{R})} \|{}_x\mathcal{D}_1^{\frac{s}{2}} v\|_{L_2(\mathbb{R})} = \|d\|_{L_\infty(\Omega)} \|{}_0\mathcal{D}_x^{\frac{s}{2}} u\|_{L_2(\mathbb{R})} \|{}_0\mathcal{D}_x^{\frac{s}{2}} v\|_{L_2(\mathbb{R})} \end{aligned}$$

yielding the bound

$$\begin{aligned} a(u, v) &\leq (\|d\|_{L_\infty(\Omega)} + \|r\|_{L_\infty(\Omega)}) (\|{}_0\mathcal{D}_x^{\frac{s}{2}} u\|_{L_2(\mathbb{R})}^2 + \|u\|_{L_2(\Omega)}^2)^{1/2} \\ &\quad \times (\|{}_0\mathcal{D}_x^{\frac{s}{2}} v\|_{L_2(\mathbb{R})}^2 + \|v\|_{L_2(\Omega)}^2)^{1/2} \\ &\leq 2 (\|d\|_{L_\infty(\Omega)} + \|r\|_{L_\infty(\Omega)}) \|u\|_{\tilde{H}^{s/2}(\Omega)} \|v\|_{\tilde{H}^{s/2}(\Omega)}, \end{aligned}$$

by Proposition 2.11, which proves the claim. \square

To prove the coercivity of the bilinear form in eq. (3.3), we need additional conditions on $d \in L_\infty(\Omega)$.

Assumption 3.4. We define the average $\mu(d)$ and the range $\varrho(d)$ of d as

$$\mu(d) := \frac{1}{2} \left(\operatorname{ess\,sup}_{x \in \Omega} d(x) + \operatorname{ess\,inf}_{x \in \Omega} d(x) \right), \quad \varrho(d) := \frac{1}{2} \left(\operatorname{ess\,sup}_{x \in \Omega} d(x) - \operatorname{ess\,inf}_{x \in \Omega} d(x) \right)$$

as well as $\underline{r} := \operatorname{ess\,inf}_{x \in \Omega} r(x)$. Setting $\gamma_{s,d} := \mu(d) |\cos(s\frac{\pi}{2})| - \varrho(d)$, we assume in addition to Assumption 3.1 that

$$c_{s,d,r} := \gamma_{s,d} \frac{\Gamma(s/2+1)^2}{4} + \underline{r} \geq 0. \quad (3.5)$$

Remark 3.5. (a) It is immediate that $\|d - \mu(d)\|_{L_\infty(\Omega)} = \varrho(d)$.

(b) As $s \rightarrow 2$, the value $|\cos(s\frac{\pi}{2})|$ converges to 1, so that $\gamma_{s,d} = \operatorname{ess\,inf}_{x \in \Omega} d(x)$. On the other hand, if $s \rightarrow 1$, the value of $\cos(s\frac{\pi}{2})$ tends to zero, which means that d can only vary very little since $\varrho(d)$ must be very small to satisfy (3.5).

The following result is a generalization of [14, Thm. 4.3] for non-constant diffusion. Moreover, we shall make the involved constants explicit for later use.

Theorem 3.6. If Assumptions 3.1 and 3.4 hold, $a(\cdot, \cdot)$ is coercive, i.e.,

$$a(u, u) \geq \alpha_{s,d} \|u\|_{\tilde{H}^{\frac{s}{2}}(\Omega)}^2, \quad u \in \tilde{H}^{\frac{s}{2}}(\Omega) \quad \text{where } \alpha_{s,d} = \gamma_{s,d} \frac{\Gamma(s/2+1)^4}{8}.$$

Moreover, Problem 3.2 admits a unique solution $u \in \tilde{H}^{\frac{s}{2}}(\Omega)$ such that

$$\|u\|_{\tilde{H}^{\frac{s}{2}}(\Omega)} \leq \frac{1}{\alpha_{s,d}} \|f\|_{L_2(\Omega)}. \quad (3.6)$$

Proof. By Lemma 2.10, we have that

$$\begin{aligned} a_1(u, u) &= -\mu(d) \left({}_0\mathcal{D}_x^{\frac{s}{2}} u, {}_x\mathcal{D}_1^{\frac{s}{2}} u \right)_{L_2(\Omega)} - \left((d - \mu(d)) {}_0\mathcal{D}_x^{\frac{s}{2}} u, {}_x\mathcal{D}_1^{\frac{s}{2}} u \right)_{L_2(\Omega)} \\ &\geq (\mu(d) |\cos(s\frac{\pi}{2})| - \varrho(d)) \|{}_0\mathcal{D}_x^{\frac{s}{2}} u\|_{L_2(\mathbb{R})}^2 = \gamma_{s,d} |u|_{s/2}^2. \end{aligned}$$

Thanks to Assumption 3.4 and by using Proposition 2.11, we get that

$$\begin{aligned} a(u, u) &\geq \gamma_{s,d} |u|_{s/2}^2 + \underline{r} \|u\|_{L_2(\Omega)}^2 \geq \gamma_{s,d} \frac{\Gamma(s/2+1)^2}{4} \|u\|_{s/2}^2 + \underline{r} \|u\|_{L_2(\Omega)}^2 \\ &\geq \gamma_{s,d} \frac{\Gamma(s/2+1)^2}{4} |u|_{s/2}^2 \geq \gamma_{s,d} \frac{\Gamma(s/2+1)^4}{8} \|u\|_{\tilde{H}^{\frac{s}{2}}(\Omega)}^2. \end{aligned}$$

Well-posedness follows from the Lax-Milgram- resp. Banach-Nečas theorem, [2, §4.5]. \square

Remark 3.7. The coercivity constant given in Theorem 3.6 does not depend on \underline{r} in Assumption 3.4, but might not be optimal depending on the value of \underline{r} . If, e.g., $\underline{r} \geq 0$, we see that $a(u, u) \geq \gamma_{s,d} \frac{\Gamma(s/2+1)^2}{2} \|u\|_{\tilde{H}^{\frac{s}{2}}(\Omega)}^2$. On the other hand, if $\underline{r} < 0$, we may argue as in the proof of Proposition 2.11 to obtain the bound $a(u, u) \geq \frac{1}{2}(\gamma_{s,d}\Gamma(s/2+1)^2 + \underline{r}) \|u\|_{\tilde{H}^{\frac{s}{2}}(\Omega)}^2$, and get an alternative form of the coercivity constant as

$$\tilde{\alpha}_{s,d,r} := \gamma_{s,d} \frac{\Gamma(s/2+1)^2}{2} + \frac{1}{2} \min\{\underline{r}, 0\}, \quad (3.7)$$

which depends on \underline{r} and might be larger than $\alpha_{s,d}$ in Theorem 3.6.

Remark 3.8. Problem 3.2 may also admit a unique solution under milder conditions replacing coercivity by an inf-sup condition, using Fredholm's alternative and/or the Peetre-Tartar lemma as in [14] for constant diffusion coefficients. We restrict ourselves here to the coercive case as it allows for an explicit formula for the coercivity constant and also since injectivity does not need to be assumed as in [14]. This is beneficial for the RBM in Section 5 as we avoid the use of the Successive Constraint Method (SCM) from [12] to compute the inf-sup condition.

3.2 Strong Solutions

For our subsequent numerical experiments, we are interested in exact solutions in order to be able to compute approximation errors exactly. To this end, we now consider strong solutions to Problem 3.2. Once again, we follow the presentation in [14, §3] (there for $d \equiv 1$) and consider the case $r(x) \equiv 0$. Their regularity will be analyzed later on. We set,

$$g(x) := {}_0\mathcal{I}_x^{\frac{s}{2}}(d(x)^{-1} {}_0\mathcal{I}_x^{\frac{s}{2}} f)(x) =: \mathcal{I}_d^s f(x),$$

so that ${}_0\mathcal{I}_x^{1-\frac{s}{2}}(d {}_0\mathcal{D}_x^{\frac{s}{2}} g) = {}_0\mathcal{I}_x^{1-\frac{s}{2}} {}_0\mathcal{I}_x^{\frac{s}{2}} f = {}_0\mathcal{I}_x^1 f$, which gives $\mathcal{D}_d^s g = f$. Next, define

$$\rho(x) := {}_0\mathcal{I}_x^{\frac{s}{2}}[d(x)^{-1} x^{\frac{s}{2}-1}], \quad p(x) := \frac{\rho(x)}{\rho(1)}. \quad (3.8)$$

Then, $p(0) = \rho(0) = 0$ and $p(1) = 1$ as well as

$$\mathcal{D}_d^s p = \frac{d}{dx} \left({}_0\mathcal{I}_x^{1-\frac{s}{2}} [d(x) {}_0\mathcal{D}_x^{\frac{s}{2}} p] \right) = \frac{1}{\rho(1)} \frac{d}{dx} \left({}_0\mathcal{I}_x^{1-\frac{s}{2}} x^{\frac{s}{2}-1} \right) = \frac{1}{\rho(1)} \frac{d}{dx} (1) = 0,$$

Hence, the strong solution of Problem 3.2 reads

$$u = -g + [(\mathcal{I}_d^s f)(1)] p. \quad (3.9)$$

It is clear that $u \in \tilde{H}^{\frac{s}{2}}(\Omega)$. In order to show that u is a solution of Problem 3.2, let $v \in C_0^\infty(\Omega)$. Then,

$$\begin{aligned} \langle \mathcal{D}_d^{\frac{s}{2}} p, v \rangle_{H^{-\frac{s}{2}}(\Omega) \times \tilde{H}^{\frac{s}{2}}(\Omega)} &= \left(d(x) {}_0\mathcal{D}_x^{\frac{s}{2}} p, {}_x\mathcal{D}_1^{\frac{s}{2}} v \right)_{L_2(\Omega)} \\ &= \frac{1}{\rho(1)} \left(d(x) d(x)^{-1} x^{\frac{s}{2}-1}, {}_x\mathcal{D}_1^{\frac{s}{2}} v \right)_{L_2(\Omega)} = \frac{1}{\rho(1)} \left(x^{\frac{s}{2}-1}, {}_x\mathcal{I}_1^{1-\frac{s}{2}} v' \right)_{L_2(\Omega)} \\ &= \frac{1}{\rho(1)} \left({}_0\mathcal{I}_x^{1-\frac{s}{2}} x^{\frac{s}{2}-1}, v' \right)_{L_2(\Omega)} = \frac{\Gamma(\frac{s}{2})}{\rho(1)} (1, v')_{L_2(\Omega)} = 0, \end{aligned} \quad (3.10)$$

where we have used Lemmas 2.4, 2.7 and 2.8 together with the fact that ${}_0\mathcal{I}_x^{1-\frac{s}{2}} x^{\frac{s}{2}-1} = \Gamma(\frac{s}{2})$ (see, e.g. [15, Prop. 2.1]). Analogously, we have that

$$\begin{aligned} \langle \mathcal{D}_d^s g, v \rangle_{H^{-\frac{s}{2}}(\Omega) \times \tilde{H}^{\frac{s}{2}}(\Omega)} &= \left(d(x) {}_0\mathcal{D}_x^{\frac{s}{2}} g, {}_x\mathcal{D}_1^{\frac{s}{2}} v \right)_{L_2(\Omega)} \\ &= \left(d(x) d(x)^{-1} {}_0\mathcal{I}_x^{\frac{s}{2}} f, {}_x\mathcal{D}_1^{\frac{s}{2}} v \right)_{L_2(\Omega)} = \left({}_0\mathcal{I}_x^{\frac{s}{2}} f, {}_x\mathcal{D}_1^{\frac{s}{2}} v \right)_{L_2(\Omega)} = (f, v)_{L_2(\Omega)}. \end{aligned} \quad (3.11)$$

Therefore, we have that by combination of eqs. (3.9) to (3.11), we have that

$$\langle \mathcal{D}_d^s u, v \rangle_{H^{-\frac{s}{2}}(\Omega) \times \tilde{H}^{\frac{s}{2}}(\Omega)} = (f, v)_{L_2(\Omega)},$$

which shows that (3.9) in fact solves Problem 3.2.

3.3 Regularity

We continue analyzing the regularity of the strong solution given in (3.9). By [15, Prop. 2.1], we have, for any $\beta > 0$,

$${}_0\mathcal{D}_x^\beta x^{\frac{s}{2}-1} = \frac{\Gamma(\frac{s}{2})}{\Gamma(\frac{s}{2}-\beta)} x^{\frac{s}{2}-\beta-1},$$

which belongs to $L_2(\Omega)$ whenever $\frac{s}{2} - \beta - 1 > -\frac{1}{2}$, i.e., $x^{\frac{s}{2}-1}$ belongs to $\tilde{H}_L^{\frac{s}{2}-\frac{1}{2}-\epsilon}(\Omega)$ for any $\epsilon > 0$. Assuming sufficient regularity of d^{-1} (e.g., $d^{-1} \in C^1(\bar{\Omega})$, see [8, La. 3.2]), we have $d^{-1}(x) x^{\frac{s}{2}-1} \in \tilde{H}_L^{\frac{s}{2}-\frac{1}{2}-\epsilon}(\Omega)$ and, by Lemma 2.3, we conclude that $p \in \tilde{H}_L^{s-\frac{1}{2}-\epsilon}(\Omega)$ (which, again, concedes with the findings in [14] for the case $d \equiv 1$). Assuming, on the other hand, $f \in L_2(\Omega)$ yields $g \in \tilde{H}_L^s(\Omega)$. Finally, arguing exactly as in the proof of [14, Thm. 4.4], yields the following result.

Theorem 3.9. *Let Assumptions 3.1 and 3.4 hold. Then, the solution u to Problem 3.2 belongs to $\tilde{H}^\beta(\Omega)$ for any $\beta \in [\frac{s}{2}, s - \frac{1}{2})$. \square*

Remark 3.10. *We note that the result in Theorem 3.9 can not be improved by assuming additional smoothness on the data f and d , since the regularity of the solution in eq. (3.9) is limited by the singular term p in eq. (3.8). Moreover, the statement remains valid for the case $r \neq 0$, even though we cannot construct the solution for this case as in Section 3.2.*

4 Finite Element Discretization

In this section, we describe and analyze a Finite Element Method (FEM) for the numerical construction of the solutions to Problem 3.2 based upon the variational formulation developed in Section 3.

To this end, we use a family of standard uniform meshes $\{\mathcal{T}_h\}_{h>0}$ with mesh-size $h > 0$ by dividing $\Omega = (0, 1)$ into $N_h \in \mathbb{N}$ sub-intervals, where $N_h > 1$ is a (possibly large) integer. We then define discrete subspaces $V_h \subset \tilde{H}^{\frac{s}{2}}(\Omega)$ of continuous and piecewise linear functions on the sub-intervals in \mathcal{T}_h . Due to the properties of $\tilde{H}^{\frac{s}{2}}(\Omega)$, we can conclude that the functions in V_h vanish at the boundaries of the domain Ω .

4.1 Error Analysis

We begin our analysis by presenting the approximation properties of the finite element space V_h as given in [14].

Lemma 4.1 ([14, La. 5.1]). *Let $\nu \in [\frac{s}{2}, 2]$, and the family of meshes $\{\mathcal{T}_h\}_{h>0}$ be quasi-uniform. If $u \in H^\nu(\Omega) \cap \tilde{H}^{\frac{s}{2}}(\Omega)$, then there exists a constant $c > 0$*

$$\inf_{v_h \in V_h} \|u - v_h\|_{\tilde{H}^{\frac{s}{2}}(\Omega)} \leq c h^{\nu-\frac{s}{2}} \|u\|_{H^\nu(\Omega)}. \quad (4.1)$$

Next, we consider the discrete version of Problem 3.2.

Problem 4.2. *Seek $u_h \in V_h$ such that $a(u_h, v_h) = F(v_h)$ holds for all $v_h \in V_h$.*

Well-posedness of Problem 4.2 is inherited from Theorem 3.6 (provided that Assumption 3.4 holds) with the coercivity constant $\alpha_{s,d}$. Moreover, we obtain the following standard a priori error bound.

Theorem 4.3. *Let Assumption 3.4 hold, then*

$$\|u - u_h\|_{\tilde{H}^{\frac{s}{2}}(\Omega)} \leq C h^{\beta^*} \|f\|_{L_2(\Omega)}$$

for any $\beta^* \in [0, \frac{s}{2} - \frac{1}{2})$ and some positive $C > 0$.

Proof. By [2, Thm. 9.42] we obtain the well-known quasi-optimality, namely $\|u_h - u\|_{\tilde{H}^{\frac{s}{2}}(\Omega)} \leq \frac{C_{d,r}}{\alpha_{s,d}} \inf_{v_h \in V_h} \|u - v_h\|_{\tilde{H}^{\frac{s}{2}}(\Omega)} \leq c \frac{C_{d,r}}{\alpha_{s,d}} h^{\nu - \frac{s}{2}} \|u\|_{H^\nu(\Omega)}$ with $C_{d,r}$ from Lemma 3.3 and $c > 0$ from Lemma 4.1. Then, Theorem 3.9 yields the estimate $\|u - u_h\|_{\tilde{H}^{\frac{s}{2}}(\Omega)} \leq Ch^{\nu - \frac{s}{2}} \|f\|_{L_2(\Omega)}$ for $\nu \in [\frac{s}{2}, s - \frac{1}{2})$ with $C > 0$ being a combination of the previous constants with Theorem 3.9. Considering $\beta^* := \nu - \frac{s}{2}$ yields the desired result. \square

Remark 4.4. As in [14, Thm. 5.3], the consideration of an adjoint problem yields the estimate

$$\|u - u_h\|_{L_2(\Omega)} + h^{\beta^*} \|u - u_h\|_{\tilde{H}^{\frac{s}{2}}(\Omega)} \leq Ch^{2\beta^*} \|f\|_{L_2(\Omega)},$$

for any $\beta^* \in [0, \frac{s}{2} - \frac{1}{2})$ and some positive $C > 0$.

4.2 The Algebraic System

As usual, a FE discretization is realized in terms of a basis, i.e., $V_h = \text{span}\{\varphi_i : i = 1, \dots, N_h - 1\}$, e.g. piecewise linear functions. Then, Problem 4.2 amounts solving a linear system of equations $\mathbf{A}_h \mathbf{u}_h = \mathbf{f}_h$, where $\mathbf{A}_h = (a(\varphi_i, \varphi_j))_{i,j=1,\dots,N_h-1} \in \mathbb{R}^{(N_h-1) \times (N_h-1)}$ is the stiffness matrix, the vector $\mathbf{f}_h = (F(\varphi_j))_{j=1,\dots,N_h-1} \in \mathbb{R}^{N_h-1}$ the right-hand side and $\mathbf{u}_h \in \mathbb{R}^{N_h-1}$ is the unknown vector of expansion coefficients of $u_h \in V_h$ in terms of the FE basis.

Due to the non-local nature of the fractional integration operator, it is clear that \mathbf{A}_h is non-symmetric and densely populated. Without any further compression, the setup of \mathbf{A}_h and any matrix-vector multiplication e.g. used within a GMRES iteration requires $\mathcal{O}(N_h^2)$ operations. Moreover, the number of GMRES iterations is known to depend on the condition number $\kappa(\mathbf{A}_h)$, which we are going to analyze next.

To this end, recall the maximum and minimum singular values

$$\sigma_{h,\max} := \sup_{\mathbf{u}_h \in \mathbb{R}^{N_h-1}} \sup_{\mathbf{v}_h \in \mathbb{R}^{N_h-1}} \varrho(\mathbf{A}_h, \mathbf{u}_h, \mathbf{v}_h), \quad \sigma_{h,\min} := \inf_{\mathbf{u}_h \in \mathbb{R}^{N_h-1}} \sup_{\mathbf{v}_h \in \mathbb{R}^{N_h-1}} \varrho(\mathbf{A}_h, \mathbf{u}_h, \mathbf{v}_h),$$

where $\varrho(\mathbf{A}_h, \mathbf{u}_h, \mathbf{v}_h) := \frac{\mathbf{v}_h^\top \mathbf{A}_h \mathbf{u}_h}{\|\mathbf{u}_h\|_2 \|\mathbf{v}_h\|_2}$ denotes the Rayleigh quotient.

Proposition 4.5. *Let Assumptions 3.1 and 3.4 hold and let V_h be spanned by piecewise linear FEs. Then, there exists a constant $c > 0$ independent of the mesh-size h such*

$$\kappa(\mathbf{A}_h) \leq c \frac{h^{-s}}{\alpha_{s,d}}.$$

Proof. Let $u_h, v_h \in V_h$ denote arbitrary elements of the discrete space and denote the vectors associated with their FE representation as \mathbf{u}_h and $\mathbf{v}_h \in \mathbb{R}^{N_h-1}$, so that $a(u_h, v_h) = \mathbf{v}_h^\top \mathbf{A}_h \mathbf{u}_h$. Then, $\sqrt{h} \|\mathbf{u}_h\|_2 \sim \|u_h\|_{L_2(\Omega)}$ independent of h for $u_h \in V_h$, where $\|\cdot\|_2$ denotes the standard Euclidean vector norm. Then, Theorem 3.6 yields

$$\begin{aligned} \sigma_{h,\min} &= \inf_{\mathbf{u}_h \in \mathbb{R}^n} \sup_{\mathbf{v}_h \in \mathbb{R}^n} \frac{\mathbf{v}_h^\top \mathbf{A}_h \mathbf{u}_h}{\|\mathbf{u}_h\|_2 \|\mathbf{v}_h\|_2} \geq \inf_{\mathbf{u}_h \in \mathbb{R}^n} \frac{\mathbf{u}_h^\top \mathbf{A}_h \mathbf{u}_h}{\|\mathbf{u}_h\|_2^2} \\ &\gtrsim h \inf_{u_h \in V_h} \frac{a(u_h, u_h)}{\|u_h\|_{L_2(\Omega)}^2} \gtrsim \alpha_{s,d} h \inf_{u_h \in V_h} \frac{\|u_h\|_{\tilde{H}^{\frac{s}{2}}(\Omega)}^2}{\|u_h\|_{L_2(\Omega)}^2} \gtrsim \alpha_{s,d} h, \end{aligned}$$

where we used e.g. [25, La. 10.5] and the involved constant is independent on the mesh-size. Next,

proceeding analogously as before and employing Lemma 3.3, we find that

$$\begin{aligned}
\sigma_{h,\max} &= \sup_{\mathbf{u}_h \in \mathbb{R}^n} \sup_{\mathbf{v}_h \in \mathbb{R}^n} \frac{\mathbf{v}_h^\top \mathbf{A}_h \mathbf{u}_h}{\|\mathbf{u}_h\|_2 \|\mathbf{v}_h\|_2} \lesssim h \sup_{u_h \in V_h} \sup_{v_h \in V_h} \frac{a(u_h, v_h)}{\|u_h\|_{L_2(\Omega)} \|v_h\|_{L_2(\Omega)}} \\
&\lesssim h C_{d,r} \sup_{u_h \in V_h} \sup_{v_h \in V_h} \frac{\|u_h\|_{\tilde{H}^{\frac{s}{2}}(\Omega)} \|v_h\|_{\tilde{H}^{\frac{s}{2}}(\Omega)}}{\|u_h\|_{L_2(\Omega)} \|v_h\|_{L_2(\Omega)}} \\
&\lesssim h C_{d,r} h^{-s} \sup_{u_h \in V_h} \sup_{v_h \in V_h} \frac{\|u_h\|_{L_2(\Omega)} \|v_h\|_{L_2(\Omega)}}{\|u_h\|_{L_2(\Omega)} \|v_h\|_{L_2(\Omega)}} \lesssim C_{d,r} h^{1-s},
\end{aligned}$$

where we have used a Bernstein-type inequality, see e.g. [25, La. 10.5, Thm. 10.7]. The claim follows from the combination of the two previous results. \square

5 The Reduced Basis Method (RBM)

In this section, we show how to apply the RBM for the above example of a *parameterized* fractional PDE (PFPDE). We built upon standard references on the RBM such as [10, 11, 21, 26], refer the reader to these and omit further references as most of what is said is rather standard.

5.1 A Parametrized Fractional PDE (PFPDE)

The model reduction techniques can in general be used in order to find the numerical solutions of PDEs depending on parameters (PPDEs). These parameters are collected in a vector $\mu \in \mathbb{P}$, with compact set $\mathbb{P} \subset \mathbb{R}^P$, $P \in \mathbb{N}$. Here, we consider a parametric version of (1.1) for $\mu \in \mathbb{P}$ defined via the parameter-dependent differential operator

$$\mathcal{A}(\mu)u := -{}_0\mathcal{D}_x^{\frac{s}{2}} \left(d(\mu) {}_0\mathcal{D}_x^{\frac{s}{2}} u \right) + r(\mu) u,$$

and right-hand side $f(\mu)$, where

$$c(\mu) = \sum_{q=1}^{Q^c} \vartheta_q^c(\mu) c_q, \quad c \in \{d, r, f\},$$

$\vartheta_q^d, \vartheta_q^r, \vartheta_q^f : \mathbb{P} \rightarrow \mathbb{R}$, $Q^d, Q^r, Q^f \in \mathbb{N}$ and $d_q, r_q \in L_\infty(\Omega)$ as well as $f_q \in L_2(\Omega)$ are given. The above representation of $d(\mu)$, $r(\mu)$ and $f(\mu)$ is known as *affine decomposition*. If such a representation is not given, one may construct an approximation by means of the *Empirical Interpolation Method (EIM)*, [4]. Then, we can write the (classical form of the) parametrized problem as

$$\mathcal{A}(\mu) u_\mu(x) = f(x; \mu), \quad x \in \Omega = (0, 1), \quad u_\mu(0) = 0, \quad u_\mu(1) = 0. \quad (5.1)$$

We shall use the above derived variational formulation of (5.1): given $\mu \in \mathbb{P}$, we seek $u_\mu \in V$ such that

$$a(u_\mu, v; \mu) = f(v; \mu) \quad \text{for all } v \in V, \quad (5.2)$$

where the parametric bilinear form $a : V \times V \times \mathbb{P} \rightarrow \mathbb{R}$ is defined as

$$a(u, v; \mu) := - \left(d(\mu) {}_0\mathcal{D}_x^{\frac{s}{2}} u, {}_x\mathcal{D}_1^{\frac{s}{2}} v \right)_{L_2(\Omega)} + (r(\mu) u, v)_{L_2(\Omega)}$$

for $u, v \in V$ and the parametric linear form $f : H \times \mathbb{P} \rightarrow V$, $H := L_2(\Omega)$, is given by $f(v; \mu) = (f(\mu; \cdot), v)_H$ for $v \in V \subset H$.

Recall, that the well-posedness of the variational problem relies on Assumption 3.4, see Theorem 3.6. By adding the parameter-dependency to the diffusion coefficient d in Assumption 3.4, we

obtain the parameter-dependent number $\gamma_{s,d}(\mu) := \mu(d(\mu)) |\cos(s\frac{\pi}{2})| - \varrho(d(\mu))$ and the condition (3.5) then reads

$$\gamma_{s,d}(\mu) \frac{\Gamma(s/2+1)^2}{4} + \underline{r}(\mu) \geq 0. \quad (5.3)$$

Correspondingly, we obtain a parameter-dependent coercivity constant, namely

$$\alpha_{s,d}(\mu) = \gamma_{s,d}(\mu) \frac{\Gamma(s/2+1)^4}{8}, \quad (5.4)$$

or the r -dependent variant

$$\tilde{\alpha}_{s,d,r}(\mu) = \gamma_{s,d}(\mu) \frac{\Gamma(s/2+1)^2}{2} + \frac{1}{2} \min\{\underline{r}(\mu), 0\}. \quad (5.5)$$

5.2 A Detailed Discretization

The next standard ingredient for the RBM is a sufficiently detailed discretization in the sense that the numerical approximation is “indistinguishable” from the exact solution – upon discretization errors, of course. This is why such an approximation is also called the “truth” solution, which is realized by a finite-dimensional subset $V^N \subset V$ of dimension $N \gg 1$, which is typically large. Then, the truth solution $u_\mu^N \in V^N$ is determined by solving the Galerkin problem

$$a(u_\mu^N, v^N; \mu) = f(v^N; \mu) \quad \text{for all } v^N \in V^N, \quad (5.6)$$

which is well-posed as long as the original problem (5.2) is so. The following error / residual-relation is well-known

$$\|u_\mu - u_\mu^N\|_V \leq \frac{1}{\alpha_{s,d}(\mu)} \sup_{v \in V} \frac{f(v; \mu) - a(u_\mu^N, v; \mu)}{\|v\|_V} =: \frac{\|\varrho_\mu^N\|_{V'}}{\alpha_{s,d}(\mu)}, \quad (5.7)$$

where the residual is defined as usual, i.e.,

$$\varrho_\mu^N(v) := f(v; \mu) - a(u_\mu^N, v; \mu) \quad \text{for } v \in V.$$

5.3 Greedy Reduced Basis Selection

Finally, one determines a reduced space by selecting certain sample values $\mu^{(i)}$, $i = 1, \dots, n$, in an offline training phase and computing the truth “snapshots”, i.e.,

$$\xi_i := u_{\mu^{(i)}}^N, \quad i = 1, \dots, n \ll N.$$

Once, these snapshots are determined, the reduced basis approximation for some given $\mu \in \mathbb{P}$ is the Galerkin projection $u_n(\mu)$ of u_μ^N onto the reduced space $V_n := \text{span}\{\xi_1, \dots, \xi_n\}$, i.e.,

$$a(u_n(\mu), v_n; \mu) = f(v_n; \mu) \quad \text{for all } v_n \in V_n, \quad (5.8)$$

and we obtain a similar error estimate as in (5.7)

$$\|u_\mu^N - u_n(\mu)\|_V \leq \frac{\|\varrho_n(\mu)\|_{(V^N)'}}{\alpha_{s,d}(\mu)} =: \Delta_n(\mu), \quad (5.9)$$

with the RB residual defined by $\varrho_n(v^N; \mu) := f(v^N; \mu) - a(u_n(\mu), v^N; \mu)$ for $v^N \in V^N$.

The error estimator $\Delta_n(\mu)$ is maximized in the training phase over a finite-dimensional training set $\mathbb{P}_{\text{train}} \subset \mathbb{P}$ to determine the sample values $\mu^{(i)}$ of the parameters. It turns out that $\Delta_n(\mu)$ is computable with complexity independent of the truth dimension N , which is termed “online efficient”. In order to realize this, first note that the residual admits an affine decomposition, see [10] for details. Then, the dual norm of the residual, i.e., $\|\varrho_n(\mu)\|_{(V^N)'}$ can be determined via

the offline computation of Riesz representations as follows: given some $\varrho \in (V^N)'$, then its Riesz representation $\hat{\varrho} \in V^N$ is computed by solving

$$(\hat{\varrho}, v^N)_V = \varrho(v^N) \quad \text{for all } v^N \in V^N, \quad (5.10)$$

and then $\|\varrho\|_{(V^N)'} = \|\hat{\varrho}\|_{V^N}$. Hence, we need to compute

$$(w, v)_V = (w, v)_{\tilde{H}^{\frac{s}{2}}(\Omega)}.$$

Owing to Proposition 2.11, we choose the inner product given by

$$\left({}_0\mathcal{D}_x^{\frac{s}{2}} w, {}_0\mathcal{D}_x^{\frac{s}{2}} v \right)_{L_2(\Omega)},$$

inducing $|\cdot|_{s/2}$, which results in a symmetric and positive definite matrix.

Remark 5.1. *If one is not (or not only) interested to control the state u_μ , but some functions of it, a primal-dual RBM can be used following the same route as in the standard RB references quoted above. This can be used for fractional-type problems as well by using the above variational formulation of a PFPDE.*

5.4 Kolmogorov n -Width

It is well-known that the error of the best possible approximation that can be achieved by the RBM is determined by the Kolmogorov n -width defined as

$$d_n(\mathcal{P}) := \inf_{\substack{V_n \subset V \\ \dim(V_n)=n}} \sup_{\mu \in \mathcal{P}} \inf_{v_n \in V_n} \|u(\mu) - v_n\|_V.$$

Since the problem is coercive, we can immediately apply [20, Thm. 3.1] and conclude that

$$d_n(\mathcal{P}) \leq C \exp\{-c n^{1/(Q^d+Q^r)}\}$$

for constants $C, c > 0$ and $Q^d, Q^r \in \mathbb{N}$ as in Section 5.1. The good news is that we may expect exponential decay as n grows. However, typically the sizes of the involved constants are not known. Moreover, we have to expect that the rate deteriorates as $s \rightarrow 1$ since the fractional problem then becomes more and more like a transport problem, where $d_n(\mathcal{P})$ is expected to decay slowly, [1, 20]. Hence, we are interested in making the dependence of the decay of $d_n(\mathcal{P})$ w.r.t. the fractional order s explicit.

Theorem 5.2. *Let $\mathcal{A}_s(\mu)u := -{}_0\mathcal{D}_x^s u + \mu u = f$ (in variational form) for $\mu \in \mathcal{P} := [0, \mu^+]$ and some $0 < \mu^+ < \infty$. Then, there exists a constant c and a constant C_s depending on s with $C_s \xrightarrow{s \rightarrow 1} \infty$, such that*

$$d_n(\mathcal{P}) \leq C_s \exp\left\{-c \frac{\alpha_s n}{|\mathcal{P}|}\right\},$$

where $\alpha_s \equiv \alpha_{1,s}$ is the coercivity constant of $-{}_0\mathcal{D}_x^s$ (i.e., for $d \equiv 1$).

Proof. We start by considering the complexification, i.e., $\mathcal{A}_s^{\mathbb{C}}(\hat{\mu})\hat{u} := -{}_0\hat{\mathcal{D}}_x^s \hat{u} + \hat{\mu} \hat{u} = \hat{f}$ for $\hat{\mu} = \nu + i\sigma$, $\hat{u} = u_1 + iu_2$, $\hat{f} = f_1 + if_2$. This can be rewritten as a system of the form $a_s(U, V) + (C(\hat{\mu})U, V)_{L_2(\Omega)^2}$, for $U = (u_1, u_2)^T$, $V = (v_1, v_2)^T$, where $a_s(U, V) := -({}_0\mathcal{D}_x^{\frac{s}{2}} u_1, {}_x\mathcal{D}_1^{\frac{s}{2}} v_1)_{L_2(\Omega)} - ({}_0\mathcal{D}_x^{\frac{s}{2}} u_2, {}_x\mathcal{D}_1^{\frac{s}{2}} v_2)_{L_2(\Omega)}$ and $C(\hat{\mu}) := \begin{pmatrix} \nu & -\sigma \\ \sigma & \nu \end{pmatrix}$. Then, $a_s(U, U) + \nu(U, U)_{L_2(\Omega)^2} \geq \alpha_s \|U\|_{\tilde{H}^{\frac{s}{2}}(\Omega)}^2 + \nu \|U\|_{L_2(\Omega)^2}^2$, which is positive for $\nu = \text{Re}(\hat{\mu}) > -\alpha_s$. In that case, the operator $\mathcal{A}_s^{\mathbb{C}}(\hat{\mu})$ is invertible.

For $V := \tilde{H}^{\frac{s}{2}}(\Omega)$ we define the solution map $\Phi_s : \mathcal{P} \rightarrow V$ by $\Phi_s(\mu) := u_s(\mu) = \mathcal{A}_s(\mu)^{-1}f$, where $u_s(\mu)$ denotes the unique solution of the variational formulation. Based upon the above

considerations, we may even allow complex-valued parameters. Hence, we consider the complexifications of these operators and define $\Psi_s : V^{\mathbb{C}} \times \mathbb{C} \rightarrow (V^{\mathbb{C}})'$ by $\Psi_s(\hat{v}, \hat{\mu}) := \mathcal{A}_s^{\mathbb{C}}(\hat{\mu}) \hat{v} - f^{\mathbb{C}}$, where $f^{\mathbb{C}} \in (V^{\mathbb{C}})'$ denotes the complexification of $f \in V'$. Note, that we can rewrite the variational form as $\Psi_s(\Phi_s(\mu), \mu) = 0$. Recall that, the operator $\partial_v \Psi_s(v, \hat{\mu}) = \mathcal{A}_s^{\mathbb{C}}(\hat{\mu})$ is invertible for all $\hat{\mu} \in \hat{\mathcal{P}} := \{\hat{\mu} \in \mathbb{C} : \operatorname{Re}(\hat{\mu}) > -\alpha_s\}$, which contains \mathcal{P} . As in [20] (and previously in [7]) we use the complex Banach space version of the implicit function theorem to deduce that the mapping $\hat{\Phi}_s : \hat{\mathcal{P}} \rightarrow V^{\mathbb{C}}$ defined as $\hat{\Phi}_s(\hat{\mu}) := \Phi_s(\operatorname{Re}(\hat{\mu}))$, can holomorphically be extended to an open neighborhood $\hat{\mathcal{P}} \subset \hat{\mathcal{O}} \subset \mathbb{C}$ (which is the reason for the notation $\hat{\Phi}_s$ by which we shall denote the extension to $\hat{\mathcal{O}}$, which still can be chosen appropriately). Now, we cover $\hat{\mathcal{P}}$ by circles. In fact, we choose centers $c_m := m \alpha_s$, $m = 1, \dots, M_s(\mu^+) := \left\lceil \frac{\mu^+}{\alpha_s} \right\rceil$ and fix the radius $r := (1 + \varepsilon)\alpha_s$ so that

$$\hat{\mathcal{P}} \subset \bigcup_{m=1}^{M_s(\mu^+)} D(c_m, r) \quad \text{and} \quad \bigcup_{m=1}^{M_s(\mu^+)} D(c_m, 2r) \subset \hat{\mathcal{O}},$$

where $D(c, r) := \{z \in \mathbb{C}^2 : |z - c| < r\}$ is the ball of radius r around c . Next, holomorphy implies analyticity, so that for all $1 \leq m \leq M_s(\mu^+)$ and all indices $\nu \in \mathbb{N}_0$ there exist functions $v_{m,\nu} \in V^{\mathbb{C}}$ such that

$$\hat{\Phi}(z) = \sum_{\nu \in \mathbb{N}_0} (z - c_m)^{\nu} v_{m,\nu}$$

converges absolutely for all $z \in D(c_m, 2r)$. Recall, that $v_{m,\nu} = \frac{\partial^{\nu}}{\partial z^{\nu}} \hat{\Phi}_s(c_m)$ and $\hat{\Phi}_s(c_m) = \Phi_s(c_m) = u_s(c_m)$ as well as $u_s(\mu) = \mathcal{A}_s(\mu)^{-1} f$ and $\|\mathcal{A}_s(\mu)^{-1}\| \leq \alpha_s^{-1}$ by coercivity. Hence, we deduce that $v_{m,\nu} \in V$ and $\|v_{m,\nu}\| \lesssim \alpha_s^{-\nu}$. Thus, the following quantity is independent of $M_s(\mu^+)$

$$\begin{aligned} C_s &:= \max_{1 \leq m \leq M_s(\mu^+)} \sup_{z \in D(c_m, r)} \left\| \sum_{\nu \in \mathbb{N}_0} 2^{\nu} (z - c_m)^{\nu} v_{m,\nu} \right\| \\ &\leq \max_{1 \leq m \leq M_s(\mu^+)} \sum_{\nu \in \mathbb{N}_0} 2^{\nu} 2^{-\nu} \|v_{m,\nu}\| < \infty. \end{aligned}$$

The term $2^{-\nu}$ can be put here since the supremum is taken over $z \in D(c_m, r)$, i.e., the half radius compared to the area of holomorphy which has a radius of $2r$. Moreover as $\alpha_s \rightarrow 0$ as $s \rightarrow 1$, we also see that C_s grows as $s \rightarrow 1$. Now, set

$$V_n := \operatorname{span} \left\{ v_{m,\nu} : m = 1, \dots, M_s(\mu^+), \nu = 0, \dots, K_n := \left\lfloor \frac{n}{M_s(\mu^+)} \right\rfloor \right\},$$

which is a subspace of V of dimension at most $n \in \mathbb{N}$. Moreover, for each $\mu \in \mathcal{P}$, we find a $m \in \{1, \dots, M_s(\mu^+)\}$ such that $\mu \in D(c_m, r)$ and define the reduced approximation by the truncated series

$$\Phi_{s,n}(\mu) := \sum_{|\nu| \leq K_n} (\mu - c_m)^{\nu} v_{m,\nu} \in V_n.$$

Finally, we estimate the error

$$\begin{aligned} \|\Phi_s(\mu) - \Phi_{s,n}(\mu)\| &= \left\| \sum_{\nu \geq K_n+1} (\mu - c_m)^{\nu} v_{m,\nu} \right\| = \left\| \sum_{\nu \geq K_n+1} 2^{-\nu} 2^{\nu} (\mu - c_m)^{\nu} v_{m,\nu} \right\| \\ &\leq C_s 2^{-(K_n+1)} \leq C_s \exp \left\{ -\frac{n \ln(2)}{M_s(\mu^+)} \right\}, \end{aligned}$$

which proves the claim. \square

Theorem 5.2 shows that the decay deteriorates as $s \rightarrow 1$. In fact, since the constants C_s and c_{Ω} are independent of \mathcal{P} , we clearly see the influence of the fractional order s in the sense that it

deteriorates the exponential decay rate, i.e., the convergence becomes slower and slower as $s \rightarrow 1$, i.e., $\alpha_s \rightarrow 0$ and C_s grows.

With some technical effort and corresponding assumptions, the statement of Theorem 5.2 can also be extended to operators of the form

$$\mathcal{A}_s(\mu) = \sum_{q=1}^{Q^d} \vartheta_q^d(\mu) D_{s,q} + \sum_{q=1}^{Q^r} \vartheta_q^r(\mu) r_q.$$

6 Numerical Experiments

In this section, we present numerical experiments complementing our theoretical results presented in Sections 4 and 5 by quantitative statements. All simulations were carried out using a C++ code developed by the authors [3]. The open source libraries Eigen [9] and BOOST [6, 23] were used for the treatment of the linear systems and numerical integration, respectively.

Based upon Proposition 2.11, we computed $|\varphi|_s = \|\mathcal{D}_x^s \varphi\|_{L_2(\mathbb{R})}$ as a quantity being equivalent to $\|\varphi\|_{\tilde{H}^s(\Omega)}$.

6.1 FEM - Solutions and Convergence

We begin with numerical experiments showcasing the convergence result in Theorem 4.3.

6.1.1 Constant Coefficients

We begin by considering, as in [14, §7.1], Problem 4.2 with $d \equiv 1$ and $r \equiv 0$, and test two different sources for which the analytical solution is known, namely

(Ex1) $f(x) := 1$, for which the solution is $u(x) := \frac{1}{\Gamma(s+1)}(x^{s-1} - x^s)$,

(Ex2) $f(x) := x(1-x)$, yielding $u(x) := \frac{1}{\Gamma(s+2)}(x^{s-1} - x^{s+1}) - \frac{1}{\Gamma(s+3)}(x^{s-1} - x^{s+2})$.

We also consider, for each case, three different values of s , namely $s_1 = 1.8$, $s_2 = 1.5$ and $s_3 = 1.2$, for which the expected convergence rates in $\tilde{H}^{\frac{s}{2}}(\Omega)$ read $\beta_i = \frac{s_i}{2} - \frac{1}{2}$ given by Theorem 4.3 are $\beta_1 = 0.4$, $\beta_2 = 0.25$ and $\beta_3 = 0.1$ (with respect to the mesh-size). The rates in $L_2(\Omega)$ should be the double, i.e., $\nu_i = 2\beta_i = s_i - 1$, i.e., $\nu_1 = 0.3$, $\nu_2 = 0.5$ and $\nu_3 = 0.2$.

Figures 1 and 2 display the numerical convergence rates for the two cases of f . As expected, the experimental convergence rates in $\tilde{H}^{\frac{s}{2}}(\Omega)$ asymptotically reach the predicted theoretical rates. However, the experimental convergence rate in the $L_2(\Omega)$ norm is higher than that displayed in Remark 4.4 (also see [14, Thm. 5.3]). In fact, instead of $\nu_i = 2\beta_i = s_i - 1$, we observe a rate of $s_i - \frac{1}{2}$. This effect was also observed and commented in [14, §§7.1.1, 7.1.2] but (to the best of our knowledge) there is no analysis explaining this behavior. We also observe a pre-asymptotic range of faster convergence that appears to depend on the fractional order s (with a longer pre-asymptotic range for larger values of s).

6.1.2 Non-Constant Coefficients

Next, we study the convergence of solutions to Problem 4.2 with non-constant diffusion and reaction coefficients d and r , respectively. We consider two different cases, namely

(Ex3) $d(x) := 4 + \sin(2\pi x)$ and $r(x) := \cos(2\pi x)$,

(Ex4) $d(x) := \begin{cases} 5, & \text{for } x < 0.5, \\ 3, & \text{for } x \geq 0.5, \end{cases}$ and $r(x) := \begin{cases} -2, & \text{for } x < 0.5, \\ 8, & \text{for } x \geq 0.5. \end{cases}$

Apparently, (Ex3) is made of smooth coefficients, whereas (Ex4) are piecewise defined functions. With reference to Assumption 3.4, we get $\mu(d) = 4$ and $\varrho(d) = 1$ in both cases, so that $\gamma_{s,d} := 4|\cos(s\frac{\pi}{2})| - 1$. This also means that the coercivity constants are identical in both cases. However, the reaction coefficients vary, in the first example we have $\underline{r} = -1$ and $\underline{r} = -2$ in the second one. This yields the fact the first example is only coercive for $s = 1.8$ and $s = 1.5$, whereas the second one only for $s = 1.8$, see Table 1.

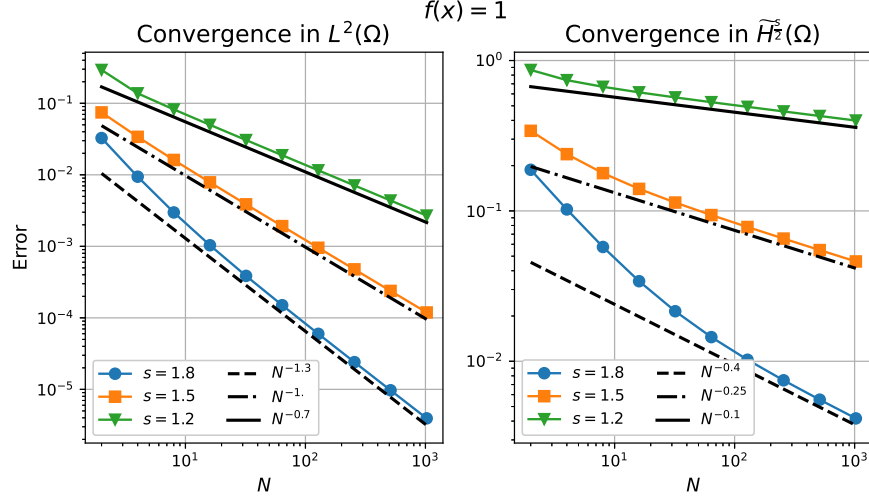


Figure 1: Convergence in the $L_2(\Omega)$ and $\tilde{H}^{\frac{s}{2}}(\Omega)$ norms to the analytical solution for the case $f(x) = 1$, (Ex1).

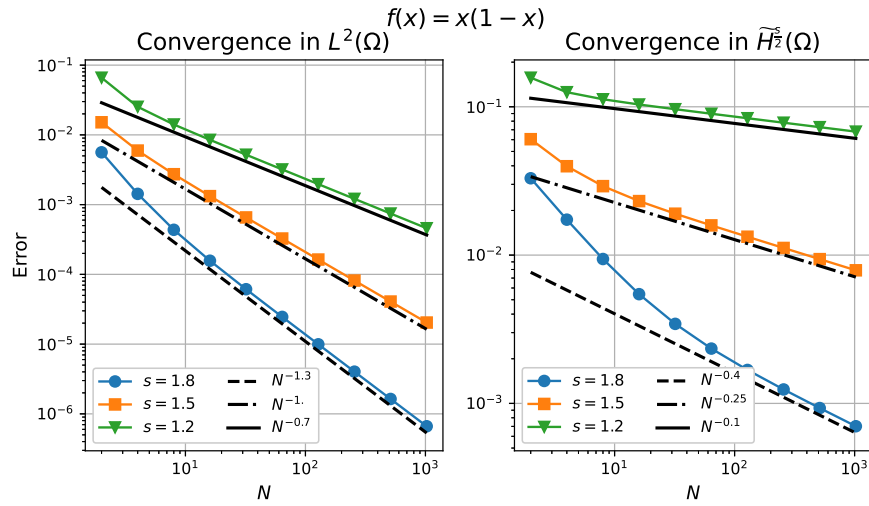


Figure 2: Convergence in the $L_2(\Omega)$ and $\tilde{H}^{\frac{s}{2}}(\Omega)$ norms to the analytical solution for the case $f(x) = x(1 - x)$, (Ex2).

(Ex3)					(Ex4)			
s	$\gamma_{s,d}$	$c_{s,d,r}$	$\alpha_{s,d}$	$\tilde{\alpha}_{s,d,r}$	s	$c_{s,d,r}$	$\alpha_{s,d}$	$\tilde{\alpha}_{s,d,r}$
1.8	2.80	1.59	0.2999	0.7969	1.8	0.59	0.2999	0.2969
1.5	1.83	0.54	0.1631	0.2722	1.5	-0.46	0.1631	-0.2278
1.2	0.24	-0.81	0.0188	-0.4058	1.2	-1.81	0.0188	-0.9058

Table 1: Involved constants for the two examples of non-constant coefficients. Left (Ex3), right (Ex4). The values for $\gamma_{s,d}$ coincide for (Ex3) and (Ex4).

We take the right-hand side $f(x) \equiv 1$ for the experiments in this subsection and compute the error against a numerically computed solution on a fine mesh. Figure 3 shows the numerical solutions. The growth of the strength of the singularity with decreasing s is apparent in both figures, while the solutions in the right graph in Figure 3 display a visible dent at the point $x = 0.5$, where the coefficients are discontinuous.

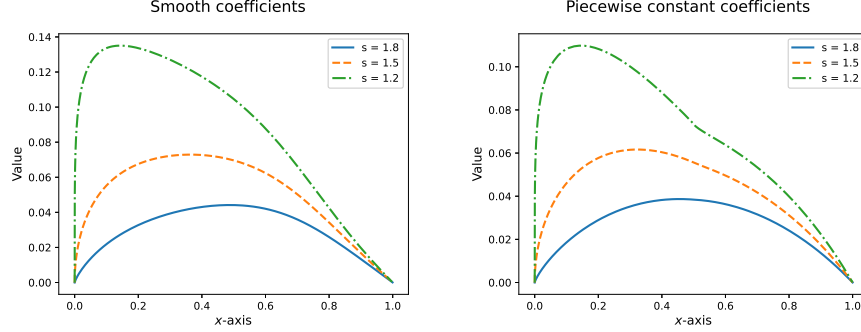


Figure 3: Numerical solutions for the case with smooth coefficients (Ex3, left) and piecewise constant coefficients (Ex4, right) for different values of s .

Figures 4 and 5 display the convergence of the discrete solutions obtained through our implementation to the respective numerically computed solutions. The figures show a behavior similar to the constant coefficient case in Section 6.1.1, with a pre-asymptotic range of faster convergence. The smoothness of the coefficients seems to play no role in the observed convergence rates, which are dominated by the singularity at the $x = 0$ endpoint. Moreover, we obtain also convergence in those cases where the bilinear form is no longer coercive, see Remark 3.8.

6.2 Conditioning of the Stiffness Matrix

We continue by presenting numerical experiments concerning Proposition 4.5. To this end, we will consider the stiffness matrices for three different problems, namely,

1. $A_h^{(1)}$ from (Ex1) or (Ex2) in Section 6.1.1;
2. $A_h^{(2)}$ corresponding to (Ex3) in Section 6.1.2;
3. $A_h^{(3)}$ corresponding to (Ex4) in Section 6.1.2.

Figure 6 displays the behavior of the singular values as the number of elements of the mesh increases (i.e., $h \rightarrow 0$). The maximum singular values display the behavior N^{s-1} , while the minimum singular values decrease as N^{-1} , as the upper bound found in Proposition 4.5. The influence of the coercivity constant is visible by the vertical offset of the curves corresponding to the same matrix.

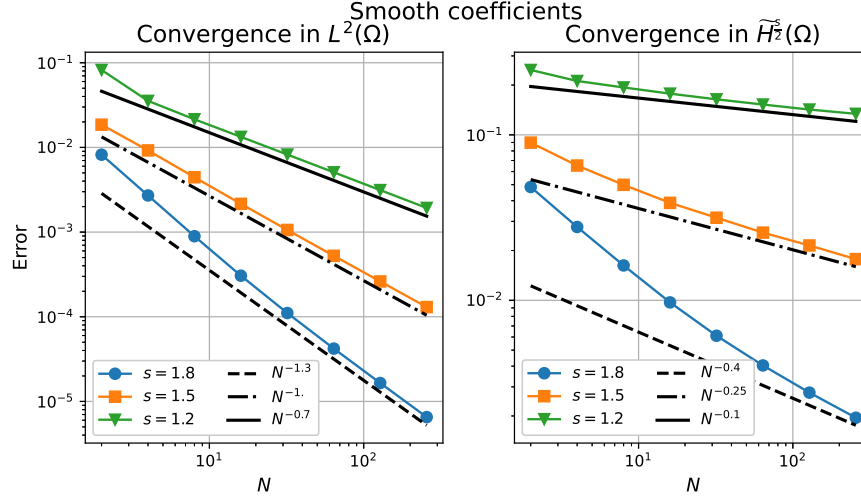


Figure 4: Convergence in the $L_2(\Omega)$ and $\tilde{H}^{\frac{s}{2}}(\Omega)$ norms to the analytical solution for the case with smooth coefficients, (Ex3).

6.3 Reduced Basis Method

Finally, we present results of our numerical experiments concerning the RBM. Our specific interest lies in the quantitative investigation of the reduction keeping in mind that the original fractional problem is nonlocal. Hence, we are interested in the decay of the greedy scheme w.r.t. the size n of the reduced system as well as in the speedup of the reduced system as compared to the full “truth” problem. For both issues, we aim at studying the dependence on the order s of the operator.

We restrict ourselves to a parameter-independent right-hand side $f(x) := x(1-x)$ and consider a parameter-dependent piecewise constant diffusion and convection coefficients given by

$$d(x; \mu) := \begin{cases} 1, & \text{if } x \in [0, 0.25), \\ \mu_1, & \text{if } x \in [0.25, 0.5), \\ \mu_2, & \text{if } x \in [0.5, 0.75), \\ \mu_3, & \text{if } x \in [0.75, 1], \end{cases} \quad \text{and} \quad r(x; \mu) := \mu_4 + \mu_5 x. \quad (6.1)$$

We choose $\mu \in \mathcal{P} := [0.7, 1.3]^3 \times [0, 1]^2 \subset \mathbb{R}^5$ and use the training set as the tensor product of 10 Gauss-Legendre quadrature points in each dimension, yielding $|\mathbb{P}_{\text{train}}| = 10^5$ training points. Again, we choose $s = 1.8, 1.5$ and 1.2 . The “truth” approximations are computed through the FEM on a uniform mesh with 2^9 elements. Since we consider here only cases where $\underline{r} \geq 0$ and we employ $|\cdot|_{s/2}$ as an equivalent norm on $\tilde{H}^{\frac{s}{2}}(\Omega)$, we use $\alpha_{s,d}$ as the associated coercivity constant (see the proof of Theorem 3.6).

6.3.1 Greedy Convergence

We determine the decay of the error of the strong greedy method for two cases, namely

1. constant diffusion ($d \equiv 1$), for which the bound in Theorem 5.2 holds;
2. the more general non-constant diffusion case (6.1).

In both cases, we expect rates of the form $d_n(\mathcal{P}) \leq C_s e^{-n \varrho_s}$. At least the constant C_s cannot easily be computed and also ϱ_s is not immediately accessible. Hence, we are interested in deriving experimental estimates for ϱ_s .

Case 1, constant diffusion: For this case, Theorem 5.2 yields $\varrho_s = c_\Omega \frac{\alpha_s}{|\mathcal{P}|}$, where here $|\mathcal{P}| = 1$ and $\alpha_s = |\cos(s\frac{\pi}{2})|$, i.e., $\alpha_{1.8} = 0.95$, $\alpha_{1.5} = 0.71$ and $\alpha_{0.12} = 0.31$. Figure 7 shows the convergence history of the greedy algorithm through the dual norm of the residual compared with

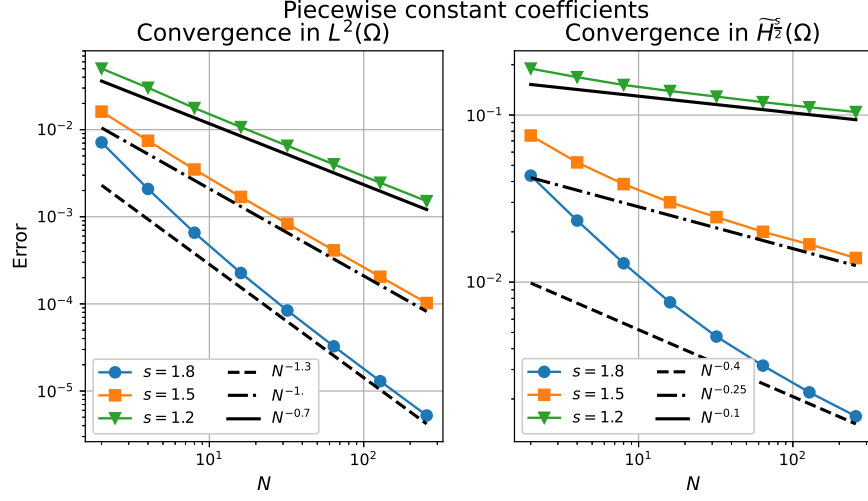


Figure 5: Convergence in the $L_2(\Omega)$ and $\tilde{H}^{\frac{s}{2}}(\Omega)$ norms to the analytical solution for the case with piecewise constant coefficients, (Ex4).

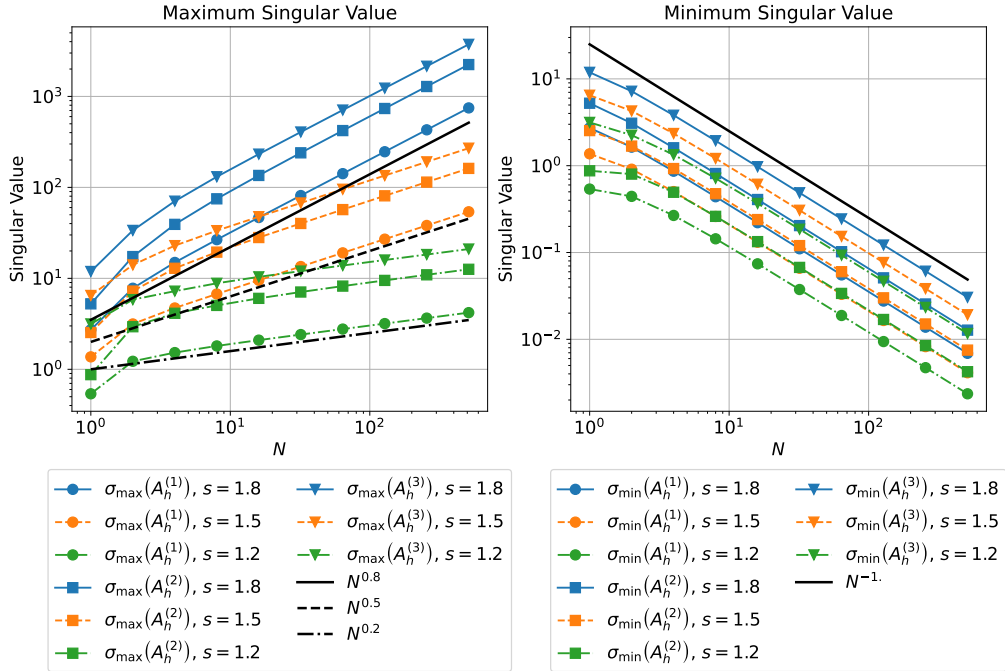


Figure 6: Maximum and minimum singular values for the different stiffness matrices and fractional orders under consideration.

the actual $\tilde{H}^{\frac{s}{2}}(\Omega)$ -error. We observe exponential rates of convergence of $\varrho_{1.8}^{\text{obs}} = 4.8$, $\varrho_{1.5}^{\text{obs}} = 4.2$ and $\varrho_{1.2}^{\text{obs}} = 3.3$, which are larger than the corresponding value of α_s – for $s \in \{1.5, 1.8\}$ by a factor of about 5, for $s = 1.2$ by a factor of about 10. We also see that the dual norm of the residual is quite close to the $\tilde{H}^{\frac{s}{2}}(\Omega)$ -error. However, for smaller s , the gap between these two values increases. If we estimate the unknown constant $c_\Omega \approx 5$ from the observed convergence rate for $s = 1.8$ and calculate the expected convergence rates at $s = 1.5$ and $s = 1.2$, we get $\varrho_{1.5} = 3.6 < 4.2 = \varrho_{1.5}^{\text{obs}}$ and $\varrho_{1.2} = 1.6 < 3.3 = \varrho_{1.2}^{\text{obs}}$, i.e., the observed rates of convergence are larger than their estimates from theory. Since this effect cannot totally be explained by the unknown constant C_s (which grows as $s \rightarrow 1+$, but whose value is unknown), we suppose a deficiency in the estimate of the coercivity constant in Theorem 3.6 for smaller values of s .

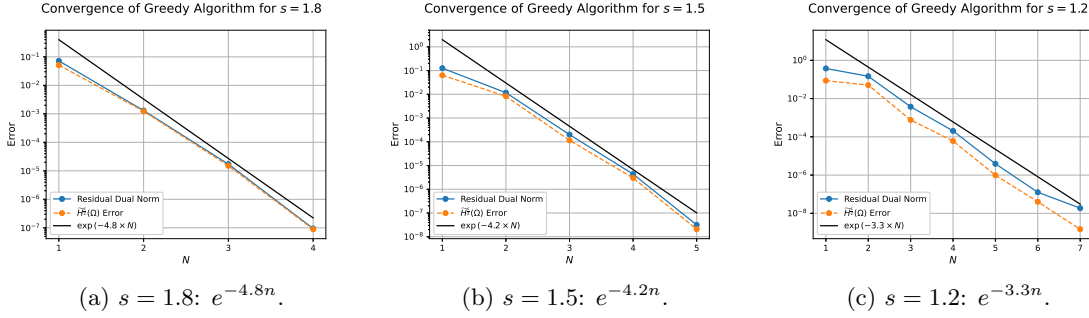


Figure 7: Convergence history of the Greedy Algorithm for the PFPDE with constant diffusion for $s \in \{1.8, 1.5, 1.2\}$.

Case 2, parameterized diffusion: For the more general case of non-constant diffusion coefficient in (6.1), we cannot apply the estimate in Theorem 5.2. Figure 8 displays the strong greedy convergence for the different cases of s . We observe exponential rates $\varrho_{1.8}^{\text{obs}} = 0.96$, $\varrho_{1.5}^{\text{obs}} = 0.76$ and $\varrho_{1.2}^{\text{obs}} = 0.65$, which (again) worsen as s approaches 1. We also display the dual norm of the residual and the actual $\tilde{H}^{\frac{s}{2}}(\Omega)$ error. Again, the gap between the two displays a dependence on the order s , worsening with decreasing values of s . This effect is even more pronounced as in Case 1. Overall, the rates are worse than in the pure reaction-case and for $s \rightarrow 1+$, we even expect to loose exponential decay (which is perfectly inlined with the known effects for the RBM for transport problems, [1, 20]).

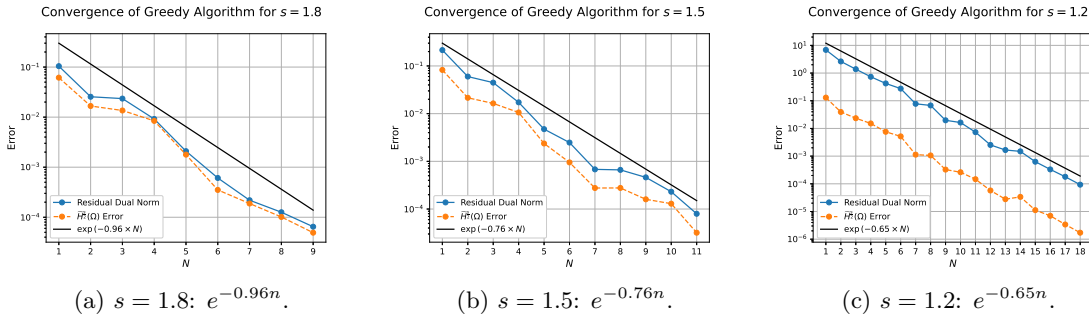


Figure 8: Convergence history of the Greedy Algorithm for the PFPDE (6.1) for $s \in \{1.8, 1.5, 1.2\}$.

6.3.2 Speedup

In addition to the improvement achieved by reducing the number of unknowns in the reduced system, there is also another possible source for reducing computational times, namely the fact that the fractional problem is non-local, i.e., the stiffness matrix is densely populated (and non-symmetric).

To this end, we consider the above Case 2 and compare computational times of the detailed versus the reduced system and determine the speedup. The results are shown in Table 2, where we compare the computational time for the resolution of a single instance of the fractional differential equation. The total achieved speedup is about 3×10^5 , mostly due to the time required to assemble the matrix for the linear system in the full-order model. If we only compare the times for solving the linear system (the affine decomposition shown in Section 5 could be used to avoid repetitive computation of the matrix), the achieved speed up is approximately 532. The computational times were obtained by solving the fractional differential equation on a uniform mesh with $2^8 = 256$ elements and using 11 elements in the reduced basis on a 2023 MacBook Air with an Apple M2 processor and 24 GB of RAM.

	FEM	RB	Ratio	Offline	
DoF	255	11	23	Affine terms	6
CPU	10 ms	18.8 μ s	532	Assembly	5.8s
				RB selection	161.6 s

Table 2: Comparison of the FEM and the RBM for Problem 3.2 (with coefficients as in eq. (6.1) and an arbitrary choice of the parameter μ).

7 Conclusions and Outlook

In this paper, we considered fractional boundary value problems involving the Riemann-Liouville fractional derivative of order $s \in (1, 2)$ with non-constant diffusion coefficients. We derived a variational formulation, proved its well-posedness and introduced a FE discretization mainly following a standard route. By parameterizing diffusion, reaction and right-hand side, we derived a parameterized fractional differential equation for which we introduced model reduction by the RBM. We proved the decay of the Kolmogorov n -width and presented results of several numerical experiments.

Some issues for future research are more or less obvious. First, we did not consider the Caputo fractional derivative as in [14]. The reason is that the Riemann-Liouville derivative puts stronger requirements on the regularity of the resulting solution, which is a more severe challenge for model reduction. Hence, we expect even better results for the Caputo derivative following the corresponding lines in [14]. We plan to investigate fractional derivatives in space and time, also involving combinations of Riemann-Liouville and Caputo derivatives.

Given data of a subdiffusive process, the rate s of subdiffusion might be unknown. In that case, one could think of using a RBM for identifying the current value of s . This means, however, that the order s would need to be a parameter. As we have seen, the solution significantly changes when s varies (and the other data stays the same), so that model reduction is expected to be tough. See, for example, [5] for such an example of model order reduction for spectral fractional diffusion problems. We devote this aspect also to future research.

8 Acknowledgments

The authors would like to thank Professors Andrea Bonito, Martin Stynes and Bangti Jin for their helpful comments and remarks on an initial version of the present manuscript. The work on this paper has been funded by the *Federal Ministry for Economic Affairs and Energy of Germany* (BMWE – Bundesministerium für Wirtschaft und Energie der Bundesrepublik Deutschland).

References

- [1] F. Arbes, C. Greif, and K. Urban. “The Kolmogorov N -width for linear transport: exact representation and the influence of the data”. In: *Adv. Comput. Math.* 51.2 (2025), Paper No. 13, 36. ISSN: 1019-7168,1572-9044.
- [2] W. Arendt and K. Urban. *Partial differential equations: an introduction to analytical and numerical methods*. Vol. 294. Springer Graduate Texts in Mathematics, 2023.
- [3] R. Aylwin. *FractionalProblem*. <https://github.com/RubenAylwin/FractionalProblem>. 2025.
- [4] M. Barrault et al. “An ‘empirical interpolation’ method: application to efficient reduced-basis discretization of partial differential equations”. In: *C. R. Math. Acad. Sci. Paris* 339.9 (2004), pp. 667–672. ISSN: 1631-073X.
- [5] A. Bonito, D. Guignard, and A. R. Zhang. “Reduced basis approximations of the solutions to spectral fractional diffusion problems”. In: *Journal of Numerical Mathematics* 28.3 (2020), pp. 147–160.
- [6] Boost C++ Libraries. *Boost C++ Libraries: Quadrature and Differentiation*. Available at: https://www.boost.org/doc/libs/1_85_0/libs/math/doc/html/quadrature.html. Accessed: 2025-05-09.
- [7] A. Cohen and R. DeVore. “Kolmogorov widths under holomorphic mappings”. In: *IMA Journal of Numerical Analysis* 36.1 (2015), pp. 1–12.
- [8] V. J. Ervin and J. P. Roop. “Variational formulation for the stationary fractional advection dispersion equation”. In: *Numerical Methods for Partial Differential Equations: An International Journal* 22.3 (2006), pp. 558–576.
- [9] G. Guennebaud, B. Jacob, et al. *Eigen v3*. <http://eigen.tuxfamily.org>. 2010.
- [10] B. Haasdonk. “Reduced Basis Methods for Parametrized PDEs — A Tutorial”. In: *Model Reduction and Approximation*. Ed. by P. Benner et al. Philadelphia: SIAM, 2017. Chap. 2, pp. 65–136.
- [11] J. S. Hesthaven, G. Rozza, and B. Stamm. *Certified Reduced Basis Methods for Parametrized Partial Differential Equations*. Cham; Heidelberg: Springer, 2016.
- [12] D. Huynh et al. “A successive constraint linear optimization method for lower bounds of parametric coercivity and inf-sup stability constants”. In: *C.R. Acad. Sci. Math.* 345.8 (2007), pp. 473–478.
- [13] B. Jin, B. Li, and Z. Zhou. “Subdiffusion with a time-dependent coefficient: analysis and numerical solution”. In: *Mathematics of Computation* 88.319 (2019), pp. 2157–2186.
- [14] B. Jin et al. “Variational formulation of problems involving fractional order differential operators”. In: *Math. Comput.* 84.296 (2015), pp. 2665–2700.
- [15] A. Kilbas. “Theory and applications of fractional differential equations”. In: *North-Holland Mathematics Studies* 204 (2006).
- [16] Y. Li, M. Jiang, and F. Liu. “Time fractional super-diffusion model and its application in peak-preserving smoothing”. In: *Chemometrics and Intelligent Laboratory Systems* 175 (2018), pp. 13–19.
- [17] Z. Mao and J. Shen. “Efficient spectral–Galerkin methods for fractional partial differential equations with variable coefficients”. In: *J. Comput. Phys.* 307 (2016), pp. 243–261.
- [18] W. C. H. McLean. *Strongly elliptic systems and boundary integral equations*. Cambridge University Press, 2000.
- [19] K. Mustapha. “FEM for time-fractional diffusion equations, novel optimal error analyses”. In: *Mathematics of Computation* 87.313 (2018), pp. 2259–2272.

- [20] M. Ohlberger and S. Rave. “Reduced Basis Methods: Success, Limitations and Future Challenges”. In: *Proceedings of ALGORITHMY* (2016), pp. 1–12.
- [21] A. Quarteroni, A. Manzoni, and F. Negri. *Reduced basis methods for partial differential equations: An introduction*. Cham; Heidelberg: Springer, 2016.
- [22] S. G. Samko. “Fractional integrals and derivatives”. In: *Theory and applications* (1993).
- [23] B. Schäling. *The boost C++ libraries*. Vol. 3. XML press Laguna Hills, 2014.
- [24] R. Schumer et al. “Eulerian derivation of the fractional advection–dispersion equation”. In: *J. Contam. Hydrol.* 48.1-2 (2001), pp. 69–88.
- [25] O. Steinbach. *Numerical approximation methods for elliptic boundary value problems: finite and boundary elements*. Springer Science & Business Media, 2007.
- [26] K. Urban. “The Reduced Basis Method in Space and Time: Challenges, Limits and Perspectives”. In: *Model Order Reduction and Applications: Cetraro, Italy 2021*. Ed. by M. Falcone and G. Rozza. Cham: Springer Nature Switzerland, 2023, pp. 1–72.
- [27] H. Wang and D. Yang. “Wellposedness of variable-coefficient conservative fractional elliptic differential equations”. In: *SIAM Journal on Numerical Analysis* 51.2 (2013), pp. 1088–1107.
- [28] S. W. Wheatcraft and M. M. Meerschaert. “Fractional conservation of mass”. In: *Adv. Water Resour.* 31.10 (2008), pp. 1377–1381.